Syntheses and characterization of α-Keggin- and α2-Dawson-type diplatinum(II)-coordinated polyoxotungstates : Effects of skeletal structure, internal element, and nitrogen-containing ligand coordinated to the platinum center for hydrogen production from water under light irradiation

Submitted to Catalysis Today Special Issue "The 8th Japan-China Workshop on Environmental Catalysis and Eco-materials"
Revised manuscript (CATTOD-D-18-00224)

Syntheses and Characterization of α-Keggin- and α_2-Dawson-type Diplatinum(II)-coordinated Polyoxotungstates: Effects of Skeletal Structure, Internal Element, and Nitrogen-containing Ligand Coordinated to the Platinum Center for Hydrogen Production from Water under Light Irradiation

Chika Nozaki Kato[a,b,*], Shunsaku Suzuki[a], Takayuki Mizuno[a], Yuki Ihara[a], Akihiro Kurihara[a], and Shunpei Nagatani[a]

[a] *Department of Chemistry, Faculty of Science, Shizuoka University, 836 Ohya, Suruga-ku, Shizuoka 422-8529, Japan*

[b] *Green Chemistry Research Division, Research Institute of Green Science and Technology, Shizuoka University, 836 Ohya, Suruga-ku, Shizuoka 422-8529, Japan*

* Corresponding author.

E-mail address: kato.chika@shizuoka.ac.jp (C. N. Kato)

ABSTRACT

The tetramethylammonium and cesium salts of diplatinum(II) complexes composed of mono-lacunary α-Keggin- and α_2-Dawson-type polyoxotungstates, $[(CH_3)_4N]_4H[\alpha\text{-}AlW_{11}O_{39}\{cis\text{-}Pt(NH_3)_2\}_2]\cdot 11H_2O$ (**TMA-AlW$_{11}$-Pt-NH$_3$**), $[(CH_3)_4N]_4H[\alpha\text{-}BW_{11}O_{39}\{cis\text{-}Pt(NH_3)_2\}_2]\cdot 9H_2O$ (**TMA-BW$_{11}$-Pt-NH$_3$**), $Cs_4[\alpha\text{-}GeW_{11}O_{39}\{Pt(bpy)\}_2]\cdot 10H_2O$ (bpy = 2,2'-bipyridine; **Cs-GeW$_{11}$-Pt-bpy**), $Cs_{3.5}H_{0.5}[\alpha\text{-}GeW_{11}O_{39}\{Pt(phen)\}_2]\cdot 3H_2O$ (phen = 1,10-phenanthroline; **Cs-GeW$_{11}$-Pt-phen**), and $Cs_6[\alpha_2\text{-}P_2W_{17}O_{61}\{cis\text{-}Pt(NH_3)_2\}_2]\cdot 13H_2O$ (**Cs-P$_2$W$_{17}$-Pt-NH$_3$**), were synthesized and characterized by X-ray crystallography, elemental analysis, TG/DTA, FTIR, and solution {^{1}H and ^{31}P} NMR spectroscopy. The characterization results showed that the two platinum(II) moieties, $[cis\text{-}Pt(NH_3)_2]^{2+}$, $[Pt(bpy)]^{2+}$, and $[Pt(phen)]^{2+}$, were coordinated to the mono-vacant site of $[XW_{11}O_{39}]^{(12-n)-}$ (X^{n+} = Al^{3+}, B^{3+}, and Ge^{4+}) and $[\alpha_2\text{-}P_2W_{17}O_{61}]^{10-}$. When the eight platinum(II) compounds, $[(CH_3)_4N]_3[\alpha\text{-}PW_{11}O_{39}\{cis\text{-}Pt(NH_3)_2\}_2]\cdot 10H_2O$ (**TMA-PW$_{11}$-Pt-NH$_3$**), $[(CH_3)_4N]_4[\alpha\text{-}SiW_{11}O_{39}\{cis\text{-}Pt(NH_3)_2\}_2]\cdot 13H_2O$ (**TMA-SiW$_{11}$-Pt-NH$_3$**), $[(CH_3)_4N]_4[\alpha\text{-}GeW_{11}O_{39}\{cis\text{-}Pt(NH_3)_2\}_2]\cdot 11H_2O$ (**TMA-GeW$_{11}$-Pt-NH$_3$**), **TMA-AlW$_{11}$-Pt-NH$_3$**, **TMA-BW$_{11}$-Pt-NH$_3$**, **Cs-GeW$_{11}$-Pt-bpy**, **Cs-GeW$_{11}$-Pt-phen**, and **Cs-P$_2$W$_{17}$-Pt-NH$_3$** were used as photocatalysts for hydrogen evolution from aqueous triethanolamine (TEOA) solution under the light irradiation, **Cs-P$_2$W$_{17}$-Pt-NH$_3$** exhibited the highest activities among the eight diplatinum(II) compounds.

Keywords Polyoxometalate • Platinum • Syntheses • Hydrogen evolution • Light irradiation

1. Introduction

The development of photocatalysts for the production of hydrogen from water is a critical issue in establishing clean energy systems [1–3]. Among the various possible photocatalysts, platinum is widely used as a co-catalyst to construct efficient photocatalytic systems for producing hydrogen because platinum promotes the separation of photo-generated electrons and holes and improves the efficiency of photocatalysis when it acts as the active center for hydrogen evolution [4]. However, platinum is expensive and of low abundance, limiting its practical application; thus, further improving the platinum utilization efficiency is an important research objective.

Polyoxometalates (POMs) are of particular interest in the fields of catalysis, surface science,

and materials science because their chemical properties including redox potentials, acidities, and solubility in various media, can be finely tuned by choosing the appropriate constituent elements and countercations [5–7]. In particular, the coordination of metal ions and organometallic fragments into the vacant site(s) of lacunary polyoxometalates is one of the most powerful techniques for constructing and stabilizing efficient and well-defined metal centers. For photocatalytic hydrogen production, several POMs have demonstrated efficient photocatalytic activities [8–13]; however, there is no report systematically investigated the influence of factors constructing the molecular structures of POMs on the photocatalytic activities.

Recently, we synthesized the cesium and tetramethylammonium salts of α-Keggin diplatinum(II)-coordinated phospho-, silico-, and germanotungstate, $Cs_3[\alpha\text{-}PW_{11}O_{39}\{cis\text{-}Pt(NH_3)_2\}_2]\cdot 8H_2O$ (**Cs-PW$_{11}$-Pt-NH$_3$**) [14], $[(CH_3)_4N]_3[PW_{11}O_{39}\{cis\text{-}Pt(NH_3)_2\}_2]\cdot 10H_2O$ (**TMA-PW$_{11}$-Pt-NH$_3$**) [15], $[(CH_3)_4N]_4[\alpha\text{-}SiW_{11}O_{39}\{cis\text{-}Pt(NH_3)_2\}_2]\cdot 13H_2O$ (**TMA-SiW$_{11}$-Pt-NH$_3$**) [16], and $[(CH_3)_4N]_4[\alpha\text{-}GeW_{11}O_{39}\{cis\text{-}Pt(NH_3)_2\}_2]\cdot 11H_2O$ (**TMA-GeW$_{11}$-Pt-NH$_3$**) [16], and successfully determined their molecular structures by X-ray crystallography. In the course of investigating the photocatalytic activities of these compounds for hydrogen evolution from aqueous triethanolamine (TEOA) solutions under light irradiation, the coordination of platinum moieties to the vacant sites in polyoxometalates was effective in improving platinum utilization efficiency, and the internal elements in α-Keggin structure affected the photocatalytic activities under the reported conditions [16,17].

In this study, we synthesized five diplatinum(II)-coordinated polyoxotungstates $[(CH_3)_4N]_4H[\alpha\text{-}AlW_{11}O_{39}\{cis\text{-}Pt(NH_3)_2\}_2]\cdot 11H_2O$ (**TMA-AlW$_{11}$-Pt-NH$_3$**), $[(CH_3)_4N]_4H[\alpha\text{-}BW_{11}O_{39}\{cis\text{-}Pt(NH_3)_2\}_2]\cdot 9H_2O$ (**TMA-BW$_{11}$-Pt-NH$_3$**), $Cs_4[\alpha\text{-}GeW_{11}O_{39}\{Pt(bpy)\}_2]\cdot 10H_2O$ (bpy = 2,2’-bipyridine; **Cs-GeW$_{11}$-Pt-bpy**), $Cs_{3.5}H_{0.5}[\alpha\text{-}GeW_{11}O_{39}\{Pt(phen)\}_2]\cdot 3H_2O$ (phen = 1,10-phenanthroline; **Cs-GeW$_{11}$-Pt-phen**), and $Cs_6[\alpha_2\text{-}P_2W_{17}O_{61}\{cis\text{-}Pt(NH_3)_2\}_2]\cdot 13H_2O$ (**Cs-P$_2$W$_{17}$-Pt-NH$_3$**) to investigate the influence of internal elements, skeletal polyoxometalate structures, and nitrogen-containing ligands on the photocatalytic activities of platinum sites for hydrogen evolution from aqueous TEOA solution under light irradiation.

2. Experimental

2.1 Materials

Cs-PW_{11}-Pt-NH_3 [14], **TMA-PW_{11}-Pt-NH_3** [15,16], **TMA-SiW_{11}-Pt-NH_3** [16], **TMA-GeW_{11}-Pt-NH_3** [16], , $K_6Na_2[\alpha\text{-}GeW_{11}O_{39}]\cdot 12H_2O$ [18], $K_9[\alpha\text{-}AlW_{11}O_{39}]\cdot 13H_2O$ [19], $K_8H[\alpha\text{-}BW_{11}O_{39}]\cdot 16H_2O$ [18,20], $K_{10}[\alpha_2\text{-}P_2W_{17}O_{61}]\cdot 23H_2O$ [21], $Pt(bpy)Cl_2$ [22], and $Pt(phen)Cl_2$ [23] were synthesized using published methods. The number of solvated water molecules was determined using thermogravimetric/differential thermal analysis (TG/DTA). All of the reagents and solvents were obtained from commercial sources and used as received.

2.2 Instrumentation/Analytical Procedures

The elemental analysis results for C, H, and N were obtained using Flash EA (Thermo Electron Corporation) at Shizuoka University (Japan). The elemental analyses results of P, B, Al, Ge, Pt, K, and Na were obtained by Optima 2100DV (PerkinElmer Inc.) at Shizuoka University (Japan), and the cesium analysis was carried out by Mikroanalytisches Labor Pascher (Germany). The Fourier transform infrared (FTIR) spectra were recorded on a Perkin Elmer Spectrum 100 FT-IR spectrometer on KBr disks at ambient temperature. The TG/DTA data were obtained using Rigaku Thermo Plus EVO2 TG/DTA 81205Z instruments in air while increasing the temperature from 20 to 500°C at a rate of 4°C/min. The ^1H (600.17 MHz) and $^{31}P\text{-}\{^1H\}$ (242.95 MHz) NMR spectra in solutions were recorded in 5-mm outer diameter tubes on a JEOL ECA-600 NMR spectrometer (Shizuoka University). The ^1H NMR spectra were measured in DMSO-d_6 with reference to an internal 3-(trimethylsilyl)-1-propanesulfonic acid sodium salt (DSS). Chemical shifts were reported as positive for resonances downfield of DSS (δ 0). The ^{31}P NMR spectra were measured in D_2O with reference to an external standard of 85% H_3PO_4 in a sealed capillary. Chemical shifts were reported as negative on the δ scale for resonances upfield of H_3PO_4 (δ 0). Solution ultraviolet-visible (UV-Vis) spectra were recorded using a Perkin-Elmer Spectrum Lambda 650 spectrophotometer.

*2.3 Synthesis and crystallization of $[(CH_3)_4N]_4H[\alpha\text{-}AlW_{11}O_{39}\{cis\text{-}Pt(NH_3)_2\}_2]\cdot 11H_2O$ (**TMA-AlW_{11}-Pt-NH_3**)*

$K_9[\alpha\text{-}AlW_{11}O_{39}]\cdot 13H_2O$ (0.665 g; 0.20 mmol) was added to a solution of *cis*-$Pt(NH_3)_2Cl_2$ (0.120 g; 0.40 mmol) dissolved in 140 mL of water. After stirring for 2 h at 60 °C, a yellow

precipitate was formed. The precipitate was removed off through a membrane filter (JG 0.2 μm), and solid $(CH_3)_4NCl$ (8.772g; 80 mmol) was added to the filtrate. After stirring for three days at 25 °C, a yellow precipitate was collected by a membrane filter (JG 0.2 μm). For purification, the crude product (0.347 g) was dissolved in water (10.4 mL) at 70 °C, followed by vapor diffusion from ethanol at 25 °C. After standing for 5 days, a yellow crystals were collected by a membrane filter (JG 0.2 μm), and washed with ethanol (10 mL). The crystallization was carried out twice. The yellow single crystals were obtained in 0.1110 g (the yield calculated on the basis of [mol of **TMA-AlW$_{11}$-Pt-NH$_3$**]/[mol of $K_9[\alpha$-$AlW_{11}O_{39}]\cdot 13H_2O] \times 100$ was 15.2%). Elemental analysis results showed: C, 5.37; H, 2.16; N, 3.07; Al, 0.65; Pt, 10.53; K, <0.1%. Calculations for $[(CH_3)_4N]_4H[AlW_{11}O_{39}\{cis$-$Pt(NH_3)_2\}_2]\cdot xH_2O$ (x = 11) = $C_{16}H_{83}N_8Pt_2O_{50}Al_1W_{11}$: C, 5.30; H, 2.31; N, 3.09; Al, 0.74; Pt, 10.76; K, 0%. TG/DTA under atmospheric conditions showed a weight loss of 5.80% with an endothermic point at 81.2 °C observed below 200.4 °C; calculations showed 5.46% for 11 water molecules. Additionally, a weight loss of 10.67% with three exothermic peaks at 261.2, 275.1, and 363.2 °C were observed in the temperature range from 245.7 to 384.4 °C; calculations showed four $[(CH_3)_4N]^+$ and four NH_3 molecules (total calcd: 10.08%). IR (KBr disk) (Fig. S1a) results in the 1800 – 400 cm^{-1} region (polyoxometalate region) showed: 1630w, 1487m, 1346w, 949s, 875s, 835s, 799s, 771s, 719s, 675m, 516m, and 459m cm^{-1}. A clear ^1H NMR spectrum could not be obtained because of its low solubility in DMSO-d_6.

*2.4 Synthesis and crystallization of $[(CH_3)_4N]_4H[\alpha$-$BW_{11}O_{39}\{cis$-$Pt(NH_3)_2\}_2]\cdot 9H_2O$ (**TMA-BW$_{11}$-Pt-NH$_3$**)*

$K_8H[\alpha$-$BW_{11}O_{39}]\cdot 16H_2O$ (0.661 g; 0.20 mmol) was dissolved in water (40 mL). The solution was added to a solution of *cis*-$Pt(NH_3)_2Cl_2$ (0.121 g; 0.40 mmol) dissolved in 150 mL of water. After stirring for 10 days at 25 °C, a yellow precipitate was formed. The precipitate was removed off through a membrane filter (JG 0.2 μm), and solid $(CH_3)_4NCl$ (3.52 g; 32.1 mmol) was added to the filtrate, and stirred for 2 h in an ice bath. Then, a yellow precipitate was collected by a membrane filter (JG 0.2 μm), and washed with a small portion of ethanol. For purification, the crude product (0.5458 g) was dissolved in waer (25 mL) at 70 °C, followed by standing in a refrigerator for 7 − 10 days. A yellow crystalline precipitate was collected by a membrane filter (JG 0.2 μm), and washed with a small portion of ethanol. The purification was

carried out twice, and the crystalline product was obtained in 0.2255 g (the yield calculated on the basis of [mol of **TMA-BW_{11}-Pt-NH_3**]/[mol of $K_8H[\alpha\text{-}BW_{11}O_{39}]\cdot 16H_2O$] × 100 was 31.5%). For the X-ray crystal measurement, the crystalline product (103.2 mg) was dissolved in water (15.5 mL) at 70 °C, followed by vapor diffusion from ethanol at 25 °C. After standing for 9 days, the yellow single crystals were obtained. Elemental analysis results showed: C, 5.32; H, 2.02; N, 3.07; B, 0.29; Pt, 10.84; K, <0.1%. Calculations for $[(CH_3)_4N]_4H[\alpha\text{-}BW_{11}O_{39}\{cis\text{-}Pt(NH_3)_2\}_2]\cdot xH_2O$ (x = 9) = $C_{16}H_{79}N_8Pt_2O_{48}B_1W_{11}$: C, 5.38; H, 2.23; N, 3.13; B, 0.30; Pt, 10.91; K, 0%. TG/DTA under atmospheric conditions showed a weight loss of 4.80% with an endothermic point at 60.5 °C observed below 101.1 °C; calculations showed 4.79% for 9 water molecules. Additionally, a weight loss of 11.40% with three exothermic peaks at 265.8, 328.2, and 421.8 °C were observed in the temperature range from 200.3 to 432.5 °C; calculations showed four $[(CH_3)_4N]^+$ and four NH_3 molecules (total calcd: 10.23%). IR (KBr disk) (Fig. S1b) results in the 1800 – 400 cm^{-1} region (polyoxometalate region) showed: 1625w, 1488m, 1359w, 1229w, 995m, 949s, 900s, 876s, 861s, 835s, 787s, 752s, 712m, and 520m cm^{-1}. A clear ^1H NMR spectrum could not be obtained because of its low solubility in DMSO-d_6.

*2.5 Synthesis of $Cs_4[\alpha\text{-}GeW_{11}O_{39}\{Pt(bpy)\}_2]\cdot 10H_2O$ (**Cs-GeW_{11}-Pt-bpy**)*

$Pt(bpy)Cl_2$ (0.0844 g; 0.20 mmol) was added to a solution of $K_6Na_2[\alpha\text{-}GeW_{11}O_{39}]\cdot 12H_2O$ (0.3286 g, 0.10 mmol) dissolved in 200 mL of water. After stirring for 2 h at 90 °C, solid CsCl (2.08 g; 12 mmol) was added to the solution, and stirred for a day at 25 °C. Then, a yellow precipitate was collected by a membrane filter (JG 0.2 μm), and washed with a small portion of ethanol. For purification, the crude product (0.3823 g) was dissolved in water (90 mL) at 80 °C, followed by standing for 9 days in a refrigerator at ca. 5 °C. A yellow precipitate was collected by a membrane filter (JG 0.2 μm). The product was obtained in 0.2861 g (the yield calculated on the basis of [mol of **Cs-GeW_{11}-Pt-bpy**]/[mol of $K_6Na_2[\alpha\text{-}GeW_{11}O_{39}]\cdot 12H_2O$] × 100 was 70.1%). Elemental analysis results showed: C, 5.91; H, 0.56; N, 1.36; Ge, 1.74; Pt, 9.48; Cs, 12.5; K, <0.1; Na, <0.1%. Calculations for $Cs_4[GeW_{11}O_{39}\{Pt(bpy)\}_2]\cdot xH_2O$ (x = 10) = $C_{20}H_{36}Cs_4N_4Pt_2O_{49}Ge_1W_{11}$: C, 5.81; H, 0.88; N, 1.36; Ge, 1.76; Pt, 9.44; Cs, 12.86; K, 0; Na, 0%. TG/DTA under atmospheric conditions showed a weight loss of 4.37% with endothermic points at 39.2 and 61.7 °C observed below 95.5 °C; calculations showed 4.36% for 10 water molecules. Additionally, a weight loss of 7.76% with an exothermic peak at 417 °C was

observed in the temperature range from 407.5 to 428.1 °C; calculations showed two bpy molecules (total calcd: 7.56%). IR (KBr disk) (Fig. S2a) results in the 1800 – 400 cm^{-1} region (polyoxometalate region) showed: 1609m, 1470w, 1454m, 1425w, 1313w, 1249w, 1164w, 950s, 884s, 844s, 821sh, 792s, 767s, 720s, 691m, 528w, and 465w cm^{-1}. ^{1}H NMR (DMSO-*d*$_6$, 24.3 °C) (Fig. S3): 7.329 (*t*), 7.409 (*t*), 7.994 (*t*), 8.063 (*t*), 8.171 (*d*), 8.206 (*d*), 8.366 (*d*), and 9.232 (*d*) ppm.

*2.6 Synthesis of $Cs_{3.5}H_{0.5}[\alpha$-$GeW_{11}O_{39}\{Pt(phen)\}_2]\cdot 3H_2O$ (**Cs-GeW$_{11}$-Pt-phen**)*

$Pt(phen)Cl_2$ (0.0905 g; 0.20 mmol) was added to a solution of $K_6Na_2[\alpha$-$GeW_{11}O_{39}]\cdot 12H_2O$ (0.3290 g, 0.10 mmol) dissolved in 200 mL of water. After stirring for 8 h at 90 °C, solid CsCl (2.08 g; 12 mmol) was added to the solution, and stirred for 2 days at 25 °C. Then, a yellow precipitate was collected by a membrane filter (JG 0.2 μm), and washed with a small portion of ethanol. For purification, the crude product (0.3626 g) was dissolved in 90 mL of water at 90 °C, followed by standing for 5 days in a refrigerator at ca. 5 °C. A yellow crystalline precipitate was collected by a membrane filter (JG 0.2 μm). The product was obtained in 0.2248 g (the yield calculated on the basis of [mol of **Cs-GeW$_{11}$-Pt-phen**]/[mol of $K_6Na_2[\alpha$-$GeW_{11}O_{39}]\cdot 12H_2O] \times 100$ was 54.9%). Elemental analysis results showed: C, 7.04; H, 0.55; N, 1.35; Ge, 1.75; Pt, 9.53; Cs, 12.0; K, <0.1; Na, <0.1%. Calculations for $Cs_{3.5}H_{0.5}[GeW_{11}O_{39}\{Pt(phen)\}_2]\cdot xH_2O$ (x = 3) = $C_{24}H_{22.5}Cs_{3.5}N_4Pt_2O_{42}Ge_1W_{11}$: C, 7.23; H, 0.57; N, 1.40; Ge, 1.82; Pt, 9.78; Cs, 11.66; K, 0; Na, 0%. TG/DTA under atmospheric conditions showed a weight loss of 2.25% with an endothermic point at 38.0 °C observed below 57.3 °C; calculations showed 1.35% for 3 water molecules. Additionally, a weight loss of 8.88% with an exothermic peak at 428 °C was observed in the temperature range from 424.0 to 443.1 °C; calculations showed two phen molecules (total calcd: 8.81%). IR (KBr disk) (Fig. S2b) results in the 1800 – 400 cm^{-1} region (polyoxometalate region) showed: 1624m, 1431m, 1412w, 1153w, 950s, 880s, 845s, 822s, 792s, 772s, 725sh, 708s, 693sh, 528w, and 470w cm^{-1}. A clear ^{1}H NMR spectrum could not be obtained because of its low solubility in DMSO and D_2O.

*2.7 Synthesis of $Cs_6[\alpha_2$-$P_2W_{17}O_{61}\{cis$-$Pt(NH_3)_2\}_2]\cdot 13H_2O$ (**Cs-P$_2$W$_{17}$-Pt-NH$_3$**)*

$K_{10}[\alpha_2\text{-}P_2W_{17}O_{61}]\cdot 23H_2O$ (0.996 g; 0.20 mmol) was added to a solution of *cis*-$Pt(NH_3)_2Cl_2$ (0.120 g; 0.40 mmol) dissolved in 160 mL of water. After stirring for 16 h at 25 ºC, a yellow precipitate was formed. The yellow precipitate was removed off through a membrane filter (JG 0.2 μm), and CsCl (2.0172 g; 12 mmol) was added to the filtrate. After stirring for two days at 25 °C, a yellow precipitate was collected by a membrane filter (JG 0.2 μm). For purification, the crude product (1.1300 g) was dissolved in water (110 mL) at 70 °C, followed by sanding for 5 days in a refrigerator at ca. 5 °C. A yellow precipitate was collected by a membrane filter (JG 0.2 μm). At this stage, the precipitate was obtained in 0.7784 g. Here, the precipitate was not a target compound containing two platinum atoms. The second precipitation was indispensable to obtain a compound containing two platinum atoms, as follows: the precipitate obtained by the first precipitation (ca. 0.5 g) was dissolved in water at 70 °C (ca. 50 mg per 10.5 mL of water). After standing for 9 days at 25 °C, the orange crystalline precipitate was obtained in 0.1310 g (the yield calculated on the basis of [mol of **Cs-P_2W_{17}-Pt-NH_3**]/[mol of $K_{10}[\alpha_2\text{-}P_2W_{17}O_{61}]\cdot 23H_2O$] × 100 was 11.6%). Elemental analysis results showed: H, 0.59; N, 0.93; P, 1.00; Pt, 6.62; Cs, 14.4; K, <0.1%. Calculations for $Cs_6[\alpha_2\text{-}P_2W_{17}O_{61}\{cis\text{-}Pt(NH_3)_2\}_2]\cdot xH_2O$ (x = 13) = $H_{38}Cs_6N_4Pt_2O_{74}P_2W_{17}$: H, 0.68; N, 0.99; P, 1.10; Pt, 6.90; Cs, 14.11; K, 0%. TG/DTA under atmospheric conditions showed a weight loss of 4.54% with an endothermic point at 49.6 °C observed below 149.8 °C; calculations showed 4.14% for 13 water molecules. Additionally, a weight loss of 1.35% with an exothermic peak at 363.0 °C was observed in the temperature range from 337.4 to 401.8 °C; calculations showed four NH_3 molecules (calcd: 1.21%). IR (KBr disk) (Fig. S4) results in the 1800 – 400 cm^{-1} region (polyoxometalate region) showed: 1615m, 1343m, 1085s, 1054m, 1027w, 1015w, 944s, 914s, 801s, 760s, 749s, and 725m cm^{-1}. ^1H NMR (DMSO-d_6, 18.9 °C) (Fig. S5): 2.53(DMSO), 3.38(H_2O), 4.20 (NH_3), 4.46 (NH_3), 4.67 (NH_3), and 4.93 (NH_3) ppm. ^{31}P NMR (DMSO-d_6, 18.9 °C) (Fig. S6): –8.58 and –13.62 ppm.

2.8 X-Ray crystallography

A yellow block crystal of **TMA-AlW_{11}-Pt-NH_3** (0.080 × 0.030 × 0.030 mm), **TMA-BW_{11}-Pt-NH_3 (space group $P2_1/n$)** (0.150 × 0.150 × 0.130 mm), and **TMA-BW_{11}-Pt-NH_3 (space group $P2_1/c$)** (0.090 × 0.070 × 0.060 mm) was mounted on a loop or MicroMount. The measurements were carried out using a Rigaku VariMax with an XtaLAB P200 diffractometer

using multi-layer mirror-monochromated Mo Kα radiation (λ = 0.71075 Å) at 153 ± 1 K. Data were collected and processed using CrystalClear, CrystalClear-SM Expert for Windows, and structural analysis was performed using CrystalStructure for Windows. The structure was solved by SHELXS-2013 and refined by SHELXL-2014 [24]. For the three platinum-coordinated polyoxoanions, 11 tungsten atoms, 2 platinum atoms, a boron atom (or an aluminum atom), 4 nitrogen atoms, and 39 oxygen atoms were clarified. The four tetramethylammonium ions were also identified; however, the solvated water molecules could not be modeled due to the disorder of the atoms. Accordingly, the residual electron density was removed using the SQUEEZE routine in PLATON [25]. We noticed that at least two polymorphisms with space group of $P2_1/n$ and $P2_1/c$ were contained in the crystals of **TMA-BW$_{11}$-Pt-NH$_3$**, as observed for **TMA-SiW$_{11}$-Pt-NH$_3$** and **TMA-GeW$_{11}$-Pt-NH$_3$** [16].

*2.9 Crystal data of **TMA-AlW$_{11}$-Pt-NH$_3$***

$C_{16}H_{83}AlN_8O_{50}Pt_2W_{11}$; M = 3627.37, *monoclinic*, space group: $P2_1/n$ (#14), a = 13.4729(10) Å, b = 24.9534(18) Å, c = 22.5873(19) Å, β = 106.9120(18)°, V = 7265.3(10) Å^3, Z = 4, D_c = 3.316 g/cm^3, μ(Mo Kα) = 212.812 cm^{-1}, R_1 = 0.0538 [$I > 2\sigma(I)$], wR_2 = 0.1413 (for all data). GOF = 1.072 [69837 total reflections and 16631 unique reflections where $I > 2\sigma(I)$]. CCDC No. 1837598.

*2.10 Crystal data of **TMA-BW$_{11}$-Pt-NH$_3$ (space group P2$_1$/n)***

$C_{16}H_{79}BN_8O_{48}Pt_2W_{11}$; M = 3575.16, *monoclinic*, space group: $P2_1/n$ (#14), a = 13.2966(8) Å, b = 25.3672(16) Å, c = 22.1518(13) Å, β = 106.2726(12)°, V = 7172.4(7) Å^3, Z = 4, D_c = 3.311 g/cm^3, μ(Mo Kα) = 215.407 cm^{-1}, R_1 = 0.0925 [$I > 2\sigma(I)$], wR_2 = 0.2607 (for all data). GOF = 1.040 [66480 total reflections and 16416 unique reflections where $I > 2\sigma(I)$]. CCDC No. 1837600.

*2.11 Crystal data of **TMA-BW$_{11}$-Pt-NH$_3$ (space group P2$_1$/c)***

$C_{16}H_{79}BN_8O_{48}Pt_2W_{11}$; M = 3575.16, *monoclinic*, space group: $P2_1/c$ (#14), a = 13.4564(15) Å, b = 24.898(3) Å, c = 22.867(3) Å, β = 106.977(3)°, V = 7327.4(15) Å^3, Z = 4, D_c = 3.241 g/cm^3, μ(Mo Kα) = 210.850 cm^{-1}, R_1 = 0.0759 [$I > 2\sigma(I)$], wR_2 = 0.2271 (for all data). GOF =

1.076 [63757 total reflections and 16706 unique reflections where $I > 2\sigma(I)$]. CCDC No. 1837599.

2.12 Photocatalytic reaction experiments

Typical photocatalytic reactions were carried out at 25°C. **TMA-PW_{11}-Pt-NH_3**, **TMA-SiW_{11}-Pt-NH_3**, **TMA-GeW_{11}-Pt-NH_3**, **TMA-AlW_{11}-Pt-NH_3**, **TMA-BW_{11}-Pt-NH_3**, **Cs-GeW_{11}-Pt-bpy**, **Cs-GeW_{11}-Pt-phen**, and **Cs-P_2W_{17}-Pt-NH_3** (0.5 and 2.0 μmol of Pt) and Eosin Y (2.5 μmol) were dissolved in 10 mL of 100 mM aqueous TEOA solution at pH 7.0. The solution was placed into a glass reaction vessel, which was connected to a Pyrex conventional closed gas circulation system (245.5 cm^3). The photoreaction was initiated by light irradiation using a 300 W Xe lamp with a cut-off filter ($\lambda = \geq 400$ nm). The evolution of H_2, O_2, CO, and CH_4 was analyzed using a gas chromatograph (thermal conductivity detector, Molecular Sieve 5A stainless columns). The samples were assigned after comparison with standard samples analyzed under the same conditions. The turnover number (TON) was calculated as 2[H_2 evolved (mol)]/[Pt atoms (mol)].

3. Results and Discussion

3.1 Syntheses and characterization of α-Keggin- and α_2-Dawson-type diplatinum(II)-coordinated polyoxotungstates

We synthesized five diplatinum(II)-coordinated POMs, $[(CH_3)_4N]_4H[\alpha\text{-}AlW_{11}O_{39}\{cis\text{-}Pt(NH_3)_2\}_2]\cdot 11H_2O$ (**TMA-AlW_{11}-Pt-NH_3**), $[(CH_3)_4N]_4H[\alpha\text{-}BW_{11}O_{39}\{cis\text{-}Pt(NH_3)_2\}_2]\cdot 9H_2O$ (**TMA-BW_{11}-Pt-NH_3**), $Cs_4[\alpha\text{-}GeW_{11}O_{39}\{Pt(bpy)\}_2]\cdot 7H_2O$ (**Cs-PW_{11}-Pt-bpy**), $Cs_{3.5}H_{0.5}[\alpha\text{-}GeW_{11}O_{39}\{Pt(phen)\}_2]\cdot 3H_2O$ (**Cs-PW_{11}-Pt-phen**), and $Cs_6[\alpha_2\text{-}P_2W_{17}O_{61}\{cis\text{-}Pt(NH_3)_2\}_2]\cdot 13H_2O$ (**Cs-P_2W_{17}-Pt-NH_3**), by a 2:1 stoichiometric reaction of platinum(II) complexes, *cis*-$Pt(NH_3)_2Cl_2$, $Pt(bpy)Cl_2$, and $Pt(phen)Cl_2$, with mono-lacunary α-Keggin- and α_2-Dawson-type polyoxotungstates, $[\alpha\text{-}XW_{11}O_{39}]^{(12-n)-}$ (X^{n+} = Al^{3+}, B^{3+}, and Ge^{4+}) and $[\alpha_2\text{-}P_2W_{17}O_{61}]^{10-}$, in an aqueous solution, as shown in equations (1) and (2). The elemental analyses and TG/DTA results were in good agreement with the calculated values for the chemical formula of **TMA-AlW_{11}-Pt-NH_3**, **TMA-BW_{11}-Pt-NH_3**, **Cs-GeW_{11}-Pt-bpy**, **Cs-GeW_{11}-Pt-**

phen, and **Cs-P_2W_{17}-Pt-NH_3** (see experimental section). These platinum compounds were finally isolated as analytically pure, yellow powder at 15%, 32%, 70%, 55%, and 12% yield, respectively.

$[\alpha\text{-}XW_{11}O_{39}]^{(12-n)-}$ (X^{n+} = Al^{3+}, B^{3+}, Ge^{4+}) + 2 YCl_2 (Y = *cis*-$Pt(NH_3)_2$, Pt(bpy), Pt(phen))

$$\rightarrow [\alpha\text{-}XW_{11}O_{39}\{Pt(Y)\}_2]^{(8-n)-} + 4Cl^- \quad (1)$$

$[\alpha_2\text{-}P_2W_{17}O_{61}]^{10-}$ + 2 *cis*-$Pt(NH_3)_2Cl_2$

$$\rightarrow [\alpha_2\text{-}P_2W_{17}O_{61}\{cis\text{-}Pt(NH_3)_2\}_2]^{6-} + 4Cl^- \quad (2)$$

For **TMA-AlW_{11}-Pt-NH_3** and **TMA-BW_{11}-Pt-NH_3**, a single crystal for X-ray crystallography was successfully obtained by vapor diffusion from water/ethanol at 25°C. The molecular structures of **TMA-AlW_{11}-Pt-NH_3** and **TMA-BW_{11}-Pt-NH_3** are illustrated in Figs. 1, 2a, S7, and S8. Selected bond lengths and angles around the platinum centers are summarized in Tables S1 – S3. The four tetramethylammonium ions were observed by X-ray crystallography; however, the hydrated water molecules could not be identified because of the disorder. The X-ray crystallography of these platinum compounds revealed that the two *cis*-platinum(II) moieties, $[cis\text{-}Pt(NH_3)_2]^{2+}$, were coordinated each to the two oxygen atoms in a mono-vacant site of $[\alpha\text{-}XW_{11}O_{39}]^{9-}$ (X^{n+} = Al^{3+} and B^{3+}) and each platinum center had distorted square-planar geometry, as previously reported for **TMA-PW_{11}-Pt-NH_3**, **TMA-SiW_{11}-Pt-NH_3**, and **TMA-GeW_{11}-Pt-NH_3** [16]. The **TMA-BW_{11}-Pt-NH_3** crystals contained at least two polymorphisms with space group of $P2_1/n$ and $P2_1/c$ (these crystals were abbreviated as **TMA-BW_{11}-Pt-NH_3 (space group $P2_1/n$)** and **TMA-BW_{11}-Pt-NH_3 (space group $P2_1/c$)**, respectively); while the **TMA-AlW_{11}-Pt-NH_3** crystals did not contain polymorphism at least for several measurements. The partial structures around the two platinum sites in **TMA-AlW_{11}-Pt-NH_3**, **TMA-BW_{11}-Pt-NH_3 (space group $P2_1/n$)**, and **TMA-BW_{11}-Pt-NH_3 (space group $P2_1/c$)** showed that the two *cis*-platinum(II) moieties were located in an asymmetric configuration, resulting in an overall C_1 symmetry. Thus, these polyoxoanions were chiral; however, both enantiomers of $[\alpha\text{-}AlW_{11}O_{39}\{cis\text{-}Pt(NH_3)_2\}_2]^{5-}$ and $[\alpha\text{-}BW_{11}O_{39}\{cis\text{-}Pt(NH_3)_2\}_2]^{5-}$ were present in equal amounts leading to a racemic mixture. The Pt···Pt distances were 3.320, 3.401, and 3.272 Å, respectively, which were longer than those of $[anti\text{-}Pt_2(\alpha\text{-}PW_{11}O_{39})_2]^{10-}$ (2.939(4) Å) and $[syn\text{-}Pt_2(\alpha\text{-}PW_{11}O_{39})_2]^{10-}$ (3.012(6) Å) [26]. With regard to **Cs-GeW_{11}-Pt-bpy**, **Cs-GeW_{11}-Pt-phen**, and **Cs-P_2W_{17}-Pt-NH_3**, a single crystal that was suitable

for X-ray crystallography could not be obtained by vapor diffusion and slow evaporation methods.

The FTIR spectra in the range of 1800 − 400 cm^{-1} of **TMA-AlW$_{11}$-Pt-NH$_3$**, **TMA-BW$_{11}$-Pt-NH$_3$**, **Cs-GeW$_{11}$-Pt-bpy**, **Cs-GeW$_{11}$-Pt-phen**, and **Cs-P$_2$W$_{17}$-Pt-NH$_3$** measured as KBr disks are shown in Figs. S1, S2, and S4. The spectral patterns of **TMA-AlW$_{11}$-Pt-NH$_3$** (1630, 1487, 1346, 949, 875, 835, 799, 771, 719, 675, 516, and 459 cm^{-1}), **TMA-BW$_{11}$-Pt-NH$_3$** (1625, 1488, 1359, 1229, 995, 949, 900, 876, 861, 835, 787, 752, 712, and 520 cm^{-1}), **Cs-GeW$_{11}$-Pt-bpy** (1609, 1470, 1454, 1425, 1313, 1249, 1164, 950, 884, 844, 821, 792, 767, 720, 691, 528, and 465 cm^{-1}), **Cs-GeW$_{11}$-Pt-phen** (1624, 1431, 1412, 1153, 950, 880, 845, 822, 792, 772, 725, 708, 693, 528, and 470 cm^{-1}), and **Cs-P$_2$W$_{17}$-Pt-NH$_3$** (1615, 1343, 1085, 1054, 1027, 1015, 944, 914, 801, 760, 749, and 725 cm^{-1}) were different from those of $K_9[\alpha\text{-}AlW_{11}O_{39}]\cdot 13H_2O$ (937, 868, 789, 756, 704, 524, 493 cm^{-1}) [19], $K_8H[\alpha\text{-}BW_{11}O_{39}]\cdot 16H_2O$ (992, 954, 889, 841, 807, 751, 630, 514, 476, 436 cm^{-1}) [18,20], $K_6Na_2[GeW_{11}O_{39}]\cdot 12H_2O$ (957, 880, 848, 799, 720, 518, and 466 cm^{-1}) [18], and $K_{10}[\alpha_2\text{-}P_2W_{17}O_{61}]\cdot 23H_2O$ (1631, 1082, 1050, 1017, 940, 922, 889, 817, 748, and 528 cm^{-1}) [21], showing that the two platinum(II) moieties were coordinated to the vacant site of $[\alpha\text{-}XW_{11}O_{39}]^{(12-n)-}$ (X^{n+} = Al^{3+}, B^{3+}, and Ge^{4+}) and $[\alpha_2\text{-}P_2W_{17}O_{61}]^{10-}$. A band at around 1630$cm^{-1}$ was due to the adsorbed water molecules. For **TMA-AlW$_{11}$-Pt-NH$_3$** and **TMA-BW$_{11}$-Pt-NH$_3$**, the band at around 1485 cm^{-1} was assigned to tetramethylammonium ions. A band observed at around 1350cm^{-1} in **TMA-AlW$_{11}$-Pt-NH$_3$**, **TMA-BW$_{11}$-Pt-NH$_3$**, and **Cs-P$_2$W$_{17}$-Pt-NH$_3$** was assigned to ammonia molecules coordinated to the platinum centers. For **Cs-GeW$_{11}$-Pt-bpy** and **Cs-GeW$_{11}$-Pt-phen**, the bands due to bpy and phen molecules were observed in the region of 1470 − 1410 cm^{-1}.

The ^{31}P NMR spectrum in DMSO-d_6 of **Cs-P$_2$W$_{17}$-Pt-NH$_3$** showed a clear two-line spectrum at −8.58 ppm and −13.62 ppm due to the two internal phosphorus atoms, confirming the purity and homogeneity of the sample, as shown in Fig. S6. The downfield resonance is assigned to the phosphorus closest to the platinum sites, whereas the upfield resonance is due to the phosphorus closer to the W_3 cap. The signal was shifted to that of $K_{10}[\alpha_2\text{-}P_2W_{17}O_{61}]\cdot 23H_2O$ (δ −6.69 and −13.88); this was also confirmed that the two platinum(II) moieties were coordinated to the vacant site of $[\alpha_2\text{-}P_2W_{17}O_{61}]^{10-}$.

The ^{1}H NMR spectrum in DMSO-d_6 of **Cs-P$_2$W$_{17}$-Pt-NH$_3$** showed four broad signals at 4.20, 4.46, 4.67, and 4.93 ppm with approximately 1:1:1:1 intensities (Fig. S5), which could be assigned to four ammonia molecules coordinated to the platinum centers. The ^{1}H NMR spectra of **TMA-AlW$_{11}$-Pt-NH$_3$** and **TMA-BW$_{11}$-Pt-NH$_3$** were quite noisy and clear signals were not

observed because of the low solubility in DMSO-d_6. **Cs-GeW$_{11}$-Pt-bpy** showed clear ^{1}H NMR signals of bpy molecules coordinated to the platinum centers in DMSO-d_6, as shown in Fig. S3a. The signals were shifted to those of Pt(bpy)Cl$_2$ (Fig. S3b), suggesting that the [Pt(bpy)]$^{2+}$ moieties were coordinated to the vacant sites in [α-GeW$_{11}$O$_{39}$]$^{8-}$. For **Cs-GeW$_{11}$-Pt-phen**, the coordination of [Pt(phen)]$^{2+}$ to the vacant site in [α-GeW$_{11}$O$_{39}$]$^{8-}$ would cause the significant broadening of signals (Fig. S9a); however, the signals were shifted to those of Pt(phen)Cl$_2$ (Fig. S9b), suggesting that the [Pt(phen)]$^{2+}$ moieties were also coordinated to the vacant sites in [α-GeW$_{11}$O$_{39}$]$^{8-}$.

The UV-Vis spectra (Fig. S10) in the range of 320 − 800 nm of **TMA-AlW$_{11}$-Pt-NH$_3$**, **TMA-BW$_{11}$-Pt-NH$_3$**, **Cs-GeW$_{11}$-Pt-bpy**, **Cs-GeW$_{11}$-Pt-phen**, and **Cs-P$_2$W$_{17}$-Pt-NH$_3$** in water showed a broad absorption band at 406 nm (ε 1291 M^{-1}cm^{-1}), 406 nm (molecular coefficient: ε 1123 M^{-1}cm^{-1}), 388 nm (ε 6525 M^{-1}cm^{-1}), 398 nm (ε 7489 M^{-1}cm^{-1}), and 426 nm (ε 1152 M^{-1}cm^{-1}); these bands were assigned to the platinum(II) moieties coordinated to the vacant site in α-Keggin- and α$_2$-Dawson-type polyoxotungstates, as previously reported for **Cs-PW$_{11}$-Pt-NH$_3$** and **TMA-PW$_{11}$-Pt-NH$_3$** [14,15]. Thus, these results showed that **TMA-AlW$_{11}$-Pt-NH$_3$**, **TMA-BW$_{11}$-Pt-NH$_3$**, **Cs-GeW$_{11}$-Pt-bpy**, **Cs-GeW$_{11}$-Pt-phen**, and **Cs-P$_2$W$_{17}$-Pt-NH$_3$** were diplatinum(II) compounds, and the estimated structures of **Cs-GeW$_{11}$-Pt-bpy**, **Cs-GeW$_{11}$-Pt-phen**, and **Cs-P$_2$W$_{17}$-Pt-NH$_3$** are shown in Figs. 2b − 2d.

(Insert here Figs. 1 and 2)

3.2 Photocatalytic activities for hydrogen evolution from TEOA aqueous solution under light irradiation

To investigate the effects of internal elements, skeletal polyoxotungstate structures, and nitrogen-containing ligands on the photocatalytic activities of diplatinum(II) sites in α-Keggin- and α$_2$-Dawson-type polyoxotungstates, the eight platinum compounds, **TMA-PW$_{11}$-Pt-NH$_3$**, **TMA-SiW$_{11}$-Pt-NH$_3$**, **TMA-GeW$_{11}$-Pt-NH$_3$**, **TMA-AlW$_{11}$-Pt-NH$_3$**, **TMA-BW$_{11}$-Pt-NH$_3$**, **Cs-GeW$_{11}$-Pt-bpy**, **Cs-GeW$_{11}$-Pt-phen**, and **Cs-P$_2$W$_{17}$-Pt-NH$_3$** (at 0.5 and 2.0 μmol Pt) were used as photocatalysts, and determined their activities for the evolution of hydrogen from 100 mM aqueous TEOA solution (pH 7.0) under light irradiation (λ = ≥400 nm) in the presence of EY. TEOA and EY was employed as an electron donor and a photosensitizer. During the photoreactions, the platinum compounds and EY were soluble in the aqueous TEOA solution,

and black particles of Pt^0 were hardly observed under the present reaction conditions. Hydrogen was formed with 100% selectivity, and O_2, CO_2, CO, and CH_4 were not detected under these reaction conditions. For the eight platinum compounds, the order of TON after 1 h was **Cs-P_2W_{17}-Pt-NH_3** >> **TMA-PW_{11}-Pt-NH_3** > **TMA-GeW_{11}-Pt-NH_3** > **TMA-SiW_{11}-Pt-NH_3** ~ **TMA-AlW_{11}-Pt-NH_3** ~ **TMA-BW_{11}-Pt-NH_3** > **Cs-GeW_{11}-Pt-bpy** ~ **Cs-GeW_{11}-Pt-phen**, as shown in Table 1 and Fig. 3. **Cs-PW_{11}-Pt-NH_3** showed similar activities to those of **TMA-PW_{11}-Pt-NH_3**; thus, the counter-ions did not affect the photocatalytic activities under the present reaction conditions. As shown in Fig. 4a, the skeletal structure (*i.e.*, Dawson-type structure) significantly contributed to the improvement of photocatalytic activities. The nitrogen-containing ligands coordinated to the platinum centers (*i.e.*, bpy and phen molecules) remarkably reduced the photocatalytic activities, and the ammonia molecules showed the highest activities among the three diplatinum(II) complexes with α-Keggin germanotungstate (Fig. 4b). The internal elements also affected to improve the activities (Fig. 4c); however, the influence was limited compared with the skeletal structure. As control experiments, platinum compounds showed no reaction in the absence of EY. $K_{10}[\alpha_2\text{-}P_2W_{17}O_{61}]\cdot 23H_2O$ (2.0 μmol)/EY (2.5 μmol) system also showed no reaction in the absence of platinum species. When H_2PtCl_6 (2.0 μmol) was added to the $K_{10}[\alpha_2\text{-}P_2W_{17}O_{61}]\cdot 23H_2O$/EY system, 55 μmol of hydrogen was evolved after 60 min (TON was 41), which was lower than those of **Cs-P_2W_{17}-Pt-NH_3**/EY system under the same reaction conditions. Cisplatin/EY system also showed lower activities than those of **Cs-P_2W_{17}-Pt-NH_3**/EY system. These results suggested that the combination of EY and platinum species was indispensable to generate hydrogen, and the coordination of [*cis*-$Pt(NH_3)_2]^{2+}$ to the vacant site in α_2-Dawson-type polyoxotungstate was the most effective to improve the platinum utilization efficiency under the present reaction conditions.

During the light irradiation, the color of TEOA solutions dissolving EY and **TMA-PW_{11}-Pt-NH_3**, **TMA-SiW_{11}-Pt-NH_3**, **TMA-GeW_{11}-Pt-NH_3**, **TMA-AlW_{11}-Pt-NH_3**, **TMA-BW_{11}-Pt-NH_3**, **Cs-GeW_{11}-Pt-bpy**, **Cs-GeW_{11}-Pt-phen** changed from red to yellow; while, the solution containing EY and **Cs-P_2W_{17}-Pt-NH_3** changed from red to dark green. The color change would be due to the decomposition of EY to a fluorescein-like species [8,27] and the formation of heteropoly blue species (abbreviated as HPB) generated by reduction of tungsten (VI) sites in polyoxometalates [8–10]. Thus, we observed the UV-Vis spectra of aqueous solution dissolving EY (2.5 μmol) and **Cs-P_2W_{17}-Pt-NH_3** (2.0 μmol Pt) in 100 mM aqueous TEOA solution at pH 7 (10 mL), and light was irradiated for 60 min. For comparison, the solution of **TMA-PW_{11}-Pt-**

NH_3 was also monitored by UV-Vis spectroscopy. Before light irradiation, both spectra were the same as those of EY; thus, the bands of the platinum compounds were not observed because they were hidden by large bands of EY. For **TMA-PW_{11}-Pt-NH_3**, a large band at approximately 520 nm was immediately sifted to approximately 490 nm, which was assigned to a fluorescein-like species [8,27], and the absorption of EY hardly remains after at least 5-min light irradiation, as shown in Fig. 5a. In contrast, the rates of decrease in absorbance for **Cs-P_2W_{17}-Pt-NH_3** were much slower than those for **TMA-PW_{11}-Pt-NH_3**, and the absorption of EY still remained even after 60-min irradiation, as shown in Fig. 5b. During the light irradiation to the solution containing EY and **TMA-PW_{11}-Pt-NH_3**, a broad absorption of HPB was also observed in the region of 600 – 800 nm, as shown in Fig. 6a [9,10]. The absorbance gradually increased with time during 60-min light irradiation; however, the absorbance at 650 nm was still 0.07 after 60 min. In contrast, **Cs-P_2W_{17}-Pt-NH_3** showed a large band at 665 nm, and the absorbance reached to 1.09 even after 5-min light irradiation, as shown in Fig. 6b. These results suggested that α_2-Dawson-type phosphotungstate had a greater effect of inhibiting decomposition of EY than α-Keggin-type phosphotungstate. Such inhibitory effects have also been reported in EY/Pt/K_5[α-SiW_{11}{$Al(OH_2)$}O_{39}]·$7H_2O$ [8] and EY/Pt/$SiW_{11}O_{39}^{8-}$/TiO_2 [13] systems. Besides that, it has been reported that polyoxotungstate units can act as electron transmitters to accelerate charge transfer between EY and Co^{2+} cations for EY/Na_7H_{10}[$Co_6(H_2O)_2(PW_9O_{34})_2(PW_9O_{34})_2(PW_6O_{26})$]·$30H_2O$ system [11]. Furthermore, there is a report that HPB acts as a photosensitizer [9,12]. Also for the EY/ **Cs-P_2W_{17}-Pt-NH_3** system, EY^* excited from EY by the light irradiation provides electrons to the polyoxotungstate unit, and water is reduced to hydrogen at the platinum sites. Although it seems that the polyoxotungstate units plays several roles as described above under the present reaction conditions, the result that K_{10}[α_2-$P_2W_{17}O_{61}$]·$23H_2O$/EY/H_2PtCl_6 system showed lower activities than those of **Cs-P_2W_{17}-Pt-NH_3**/EY system suggested that the coordination of [*cis*-$Pt(NH_3)_2]^{2+}$ to the mono-vacant site in α_2-Dawson-type polyoxotungstate was the most effective to enhance the photocatalytic activities of diplatinum(II) compounds. Further studies regarding the reaction mechanism are in progress, and it will be reported elsewhere.

(Insert here Table 1 and Figs 3 – 6)

4. Conclusion

Five diplatinum(II) complexes composed of mono-lacunary α-Keggin- and α_2-Dawson-type polyoxotungstates, $[(CH_3)_4N]_4H[\alpha\text{-}AlW_{11}O_{39}\{cis\text{-}Pt(NH_3)_2\}_2]\cdot 11H_2O$ (**TMA-AlW$_{11}$-Pt-NH$_3$**), $[(CH_3)_4N]_4H[\alpha\text{-}BW_{11}O_{39}\{cis\text{-}Pt(NH_3)_2\}_2]\cdot 9H_2O$ (**TMA-BW$_{11}$-Pt-NH$_3$**), $Cs_4[\alpha\text{-}GeW_{11}O_{39}\{Pt(bpy)\}_2]\cdot 7H_2O$ (**Cs-PW$_{11}$-Pt-bpy**), $Cs_{3.5}H_{0.5}[\alpha\text{-}GeW_{11}O_{39}\{Pt(phen)\}_2]\cdot 3H_2O$ (**Cs-PW$_{11}$-Pt-phen**), and $Cs_6[\alpha_2\text{-}P_2W_{17}O_{61}\{cis\text{-}Pt(NH_3)_2\}_2]\cdot 13H_2O$ (**Cs-P$_2$W$_{17}$-Pt-NH$_3$**), were synthesized by a 2:1 stoichiometric reaction of platinum(II) complexes, *cis*-$Pt(NH_3)_2Cl_2$, $Pt(bpy)Cl_2$, and $Pt(phen)Cl_2$, with mono-lacunary α-Keggin- and α_2-Dawson-type polyoxotungstates, $[\alpha\text{-}XW_{11}O_{39}]^{(12-n)-}$ (X^{n+} = Al^{3+}, B^{3+}, and Ge^{4+}) and $[\alpha_2\text{-}P_2W_{17}O_{61}]^{10-}$, in an aqueous solution, and characterized by X-ray structure analysis, elemental analysis, TG/DTA, FTIR, UV-Visible, and {^{1}H and ^{31}P} solution NMR spectroscopy. We successfully obtained single crystals of **TMA-AlW$_{11}$-Pt-NH$_3$** and **TMA-BW$_{11}$-Pt-NH$_3$** by vapor diffusion from water/ethanol. The crystals of **TMA-BW$_{11}$-Pt-NH$_3$** contained at least two polymorphisms with space group of $P2_1/n$ and $P2_1/c$. Single-crystal X-ray structure analyses of the two platinum compounds revealed that the two *cis*-platinum(II) moieties, $[cis\text{-}Pt(NH_3)_2]^{2+}$, were coordinated each to two oxygen atoms in a mono-vacant site of $[XW_{11}O_{39}]^{(12-n)-}$ (X^{n+} = Al^{3+} and B^{3+}). Furthermore, the photocatalytic hydrogen production from aqueous TEOA solution under the light irradiation was carried out using a total eight platinum(II) compounds obtained by adding $[(CH_3)_4N]_3[\alpha\text{-}PW_{11}O_{39}\{cis\text{-}Pt(NH_3)_2\}_2]\cdot 10H_2O$ (**TMA-PW$_{11}$-Pt-NH$_3$**), $[(CH_3)_4N]_4[\alpha\text{-}SiW_{11}O_{39}\{cis\text{-}Pt(NH_3)_2\}_2]\cdot 13H_2O$ (**TMA-SiW$_{11}$-Pt-NH$_3$**), and $[(CH_3)_4N]_4[\alpha\text{-}GeW_{11}O_{39}\{cis\text{-}Pt(NH_3)_2\}_2]\cdot 11H_2O$ (**TMA-GeW$_{11}$-Pt-NH$_3$**) to the five platinum compounds as photocatalysts to investigate the effects of internal elements, skeletal polyoxotungstate structures, and nitrogen-containing ligands on the photocatalytic activities of diplatinum(II) centers in α-Keggin- and α_2-Dawson-type polyoxotungstates. The order of TON after 1 h was **Cs-P$_2$W$_{17}$-Pt-NH$_3$** >> **TMA-PW$_{11}$-Pt-NH$_3$** > **TMA-GeW$_{11}$-Pt-NH$_3$** > **TMA-SiW$_{11}$-Pt-NH$_3$** ~ **TMA-AlW$_{11}$-Pt-NH$_3$** ~ **TMA-BW$_{11}$-Pt-NH$_3$** > **Cs-GeW$_{11}$-Pt-bpy** ~ **Cs-GeW$_{11}$-Pt-phen**, and the skeletal structure (*i.e.*, Dawson-type structure) significantly contributed to the improvement of photocatalytic activities. The rates of EY decomposition and HPB formation were also influenced by the skeletal structure, and **Cs-P$_2$W$_{17}$-Pt-NH$_3$** suppressed the decomposition of EY, with faster formation of HPB compared with **TMA-PW$_{11}$-Pt-NH$_3$**. The result that $K_{10}[\alpha_2\text{-}P_2W_{17}O_{61}]\cdot 23H_2O$/EY/$H_2PtCl_6$ system showed lower activities than those of **Cs-P$_2$W$_{17}$-Pt-NH$_3$**/EY system suggested that the coordination of $[cis\text{-}Pt(NH_3)_2]^{2+}$ to the vacant site in α_2-Dawson-type polyoxotungstate was the most effective to improve the platinum utilization

efficiency under the present reaction conditions.

Acknowledgments

This work was supported by the Ministry of Education, Culture, Sports, Science and Technology of Japan. CNK is grateful for the support of Gender Equality Promotion Office at Shizuoka University (Japan) and Toukai Foundation for Technology (Japan). We also acknowledge Mr. Shota Hattori (Shizuoka University) for preliminary experiments regarding the synthesis of α_2-Dawson-type diplatinum(II)-coordinated polyoxotungstate.

References

[1] J. Willkomm, K. L. Orchard, A. Reynal, E. Pastor, J. R. Durrant, E. Reisner, Dye-sensitised semiconductors modified with molecular catalysts for light-driven H_2 production, Chem. Soc. Rev. 45 (2016) 9–23.

[2] K. C. Christoforidis, P. Fornasiero, Photocatalytic hydrogen production: a rift into the future energy supply, ChemCatChem 9 (2917) 1523–1544.

[3] R. Abe, Recent progress on photocatalytic and photoelectrochemical wter splitting under visible light irradiation, J. Photochem. Photobiol. C: Photochem. Rev. 11 (2010) 179–209.

[4] J. Yang, D. Wang, H. Han, C. Li, Roles of cocatalysts in photocatalysis and photoelectrocatalysis. Acc. Chem. Res. 46 (2013) 1900–1090.

[5] M. T. Pope, Heteropoly and Isopoly Oxometalates, Springer-Verlag, Berlin, 1983.

[6] M. T. Pope, A. Müller, Chemistry of polyoxometallates. Actual variation on an old theme with interdisciplinary references, Angew. Chem. Int. Ed. Engl. 30 (1991) 34–48.

[7] M. T. Pope and A. Müller (Eds.), Polyoxometalates: From Platonic Solids to Anti-Retroviral Activity, Kluwer Academic Publishers, Dordrecht, The Netherlands, 1994.

[8] X. Liu, Y. Li, S. Peng, G. Lu, S. Li, Photocatalytic hydrogen evolution under visible light irradiation by the polyoxometalate α-$[AlSiW_{11}(H_2O)O_{39}]^{5-}$-Eosin Y system, Int. J. Hydrogen Energy 37 (2012) 12150–12157.

[9] N. Fu, G. Lu, Photo-catalytic H_2 evolution over a series of Keggin-structure heteropoly bule sensitized Pt/TiO_2 under visible light irradiation, Appl. Surf. Sci. 255 (2009) 4378–4383.

[10] E. Papaconstantinou, Photochemistry of polyoxometallates of molybdenum and tungsten and/or vanadium, Chem. Soc. Rev. 18 (1989) 1–31.

[11] W. Wu, T. Teng, X-Y. Wu, X. Dui, L. Zhang, J. Xiong, L. Wu, C.-Z. Lu, A cobalt-based polyoxometalate catalyst for efficient visible-light-driven H_2 evolution from water splitting,

Catal. Commun. 64 (2015) 44–47.
[12] R. Sivakumar, J. Thomas, M. Yoon, Polyoxometalate-based molecular/nano composites: advances in environmental remediation by photocatalysis and biomimetic approaches to solar energy conversion, J. Photochem. Photobiol. C: Photochem. Rev. 13 (2012) 277–298.
[13] X. Liu, Y. Li, S. Peng, G. Lu, S. Li, Photosensitization of $SiW_{11}O_{39}^{8-}$-modified TiO_2 by Eosin Y for stable visible-light H_2 generation, Int. J. Hydrogen Energy 38 (2013) 11709–11719.
[14] C. N. Kato, Y. Morii, S. Hattori, R. Nakayama, Y. Makino, H. Uno, Diplatinum(II)-coordinated polyoxotungstate: synthesis, molecular structure, and photocatalytic performance for hydrogen evolution from water under visible-light irradiation, Dalton Trans. 41 (2012) 10021–10027.
[15] M. Kato, C. N. Kato, A Keggin-type polyoxotungstate-coordinated diplatinum(II) complex: synthesis, characterization, and stability of the *cis*-platinum(II) moieties in dimethylsulfoxide and water, Inorg. Chem. Commun. 14 (2011) 982–985.
[16] C. N. Kato, S. Suzuki, Y. Ihara, K. Aono, R. Yamashita, K. Kikuchi, T. Okamoto, H. Uno, Hydrogen evolution from water under visible-light irradiation using Keggin-type platinum(II)-coordinated phospho-, silico-, and germanotungstates as co-catalysts, Modern Res. Catal. 5 (2016) 103–129.
[17] S. Hattori, Y. Ihara, C. N. Kato, A novel photocatalytic system constructed using eosin Y, titanium dioxide, and Keggin-type platinum(II)- and aluminum(III)-coordinated polyoxotungstates for hydrogen production from water under visible light irradiation, Catal. Lett. 145 (2015) 1703–1709.
[18] N. Haraguchi, Y. Okaue, T. Isobe, Y. Matsuda, Stabilization of tetravalent cerium upon coordination of unsaturated heteropolytungstate anions. Inorg. Chem. 33 (1994) 1015–1020.
[19] J. J. Cowan, C. L. Hill, R. S. Reiner, I. A. Weinstock, W. Klemperer, K. Marek, Syntheses of selected supramolecules. Dodecatungstoaluminic acid and its monolacunary and mixed-addendum derivatives, Inorg. Synth. 33 (2002) 18–26.
[20] A. Tézé, M. Michelon, G. Hervé, Syntheses and structures of the tungstoborate anions, Inorg. Chem. 36 (1997) 505–509.
[21] D. K. Lyon, W. K. Miller, T. Novet, P. J. Domaille, E. Evitt, D. C. Johnson, R. G. Finke, Highly oxidation resistant inorganic-porphyrin analogue polyoxometalate oxidation catalysts. 1. the synthesis and characterization of aqueous-soluble potassium salts of α_2-$P_2W_{17}O_{61}(M^{n+}{\cdot}OH_2)^{(n-10)}$ and organic solvent soluble tetra-*n*-butylammonium salts of α_2-$P_2W_{17}O_{61}(M^{n+}{\cdot}Br)^{(n-11)}$ (M = Mn^{3+}, Fe^{3+}, Co^{2+}, Ni^{2+}, Cu^{2+}), J. Am. Chem. Soc. 113 (1991)

7209–7221.
[22] G. T. Morgan, F. H. Burstall, Researches on residual affinity and co-ordination. Part XXXIV. 2:2'-dipyidyl platinum salts, J. Chem. Soc. (1934) 965–971.
[23] F. A. Palocsay, J. V. Rund, The reaction between 1,10-phenanthroline and platinum(II) compounds. I. the reaction in aqueous solution, Inorg. Chem. 8 (1969) 524–528.
[24] G. M. Sheldrick, A short history of SHELX. Acta Crystallogr. A64 (2008) 112–122.
[25] A. L. Spek, Structure validation in chemical crystallography. Acta Crystallogr. D65 (2009) 148–155.
[26] Z. Lin, N. V. Izarova, A. Kondinski, X. Xing, A. Haider, L. Fan, N. Vankova, T. Heine, B. Keita, J. Cao, C. Hu, U. Kortz, Platinum-containing polyoxometalates: *syn*- and *anti*-$[Pt^{II}_2(\alpha\text{-}PW_{11}O_{39})_2]^{10-}$ and formation of the metal-metal-bonded di-Pt^{III} derivatives, Chem. Eur. J. 22 (2016) 5514–5519.
[27] K. Kimura, T. Miwa, M. Imamura, The radiolysis and photolysis of methanolic solutions of Eosin. I. the γ-radiolysis of neutral and alkaline solutions. Bull. Chem. Soc. Jpn. 43 (1970) 1329–1336.

Figure captions

Fig. 1. X-ray crystal structure (ORTEP drawing) of **TMA-AlW$_{11}$-Pt-NH$_3$**.

Fig. 2. Polyhedral representations of polyoxoanions (a) [α-$XW_{11}O_{39}${*cis*-$Pt(NH_3)_2$}$_2$]$^{(8-n)-}$ (X^{n+} = P^{5+}, Si^{4+}, Ge^{4+}, Al^{3+}, and B^{3+}), (b) [α-$GeW_{11}O_{39}${$Pt(bpy)$}$_2$]$^{4-}$, (c) [α-$GeW_{11}O_{39}${$Pt(phen)$}$_2$]$^{4-}$, and (d) [α_2-$P_2W_{17}O_{61}${*cis*-$Pt(NH_3)_2$}$_2$]$^{6-}$. The WO_6 and XO_4 units are represented by white octahedron and red tetrahedron, respectively.

Fig. 3. Time course for hydrogen evolution from aqueous TEOA solution catalyzed by platinum compounds and EY under light irradiation. Reaction conditions are shown in Table 1.

Fig. 4. The effects of (a) skeletal structure (*i.e.*, Keggin- and Dawson-type structure) in diplatinum-coordinated phosphotungstates (**TMA-PW$_{11}$-Pt-NH$_3$** and **Cs-P$_2$W$_{17}$-Pt-NH$_3$**), (b) nitrogen-containing ligand coordinated to the platinum center in diplatinum-coordinated germanotungstates (**TMA-GeW$_{11}$-Pt-NH$_3$**, **Cs-GeW$_{11}$-Pt-bpy**, and **Cs-GeW$_{11}$-Pt-phen**), and (c) internal element in α-Keggin-type polyoxotungstates (**TMA-PW$_{11}$-Pt-NH$_3$**, **TMA-SiW$_{11}$-Pt-NH$_3$**, **TMA-GeW$_{11}$-Pt-NH$_3$**, **TMA-AlW$_{11}$-Pt-NH$_3$**, and **TMA-BW$_{11}$-Pt-NH$_3$**) for hydrogen evolution from an aqueous TEOA solution under the light irradiation. Reaction conditions are shown in Table 1. The reaction time was 60 min.

Fig. 5. UV-Vis spectra in 100 mM aqueous TEOA solution at pH 7 of (a) **TMA-PW$_{11}$-Pt-NH$_3$** (1.0×10^{-4} M) and (b) **Cs-P$_2$W$_{17}$-Pt-NH$_3$** (1.0×10^{-4} M) in the presence of EY (2.5×10^{-4} M) during light irradiation for 60 min. EY and fluorescein-like species were observed at around 520 and 490 nm, respectively.

Fig. 6. UV-Vis spectra in 100 mM aqueous TEOA solution at pH 7 of (a) **TMA-PW$_{11}$-Pt-NH$_3$** (1.0×10^{-4} M) and (b) **Cs-P$_2$W$_{17}$-Pt-NH$_3$** (1.0×10^{-4} M) in the presence of EY (2.5×10^{-4} M) during light irradiation for 60 min. The HPB were observed at around 650 and 665 nm for **TMA-PW$_{11}$-Pt-NH$_3$** and **Cs-P$_2$W$_{17}$-Pt-NH$_3$**.

Table 1. Hydrogen evolution from TEOA aqueous solution under visible light irradiation[a]

Platinum compounds	Pt (μmol)	Reaction time (min)	H_2 evolved (μmol)	TON[b]	TOF[c] (h^{-1})
TMA-PW_{11}-Pt-NH_3	0.5	15	9.82	39	156
		60	38.6	154	
TMA-SiW_{11}-Pt-NH_3		15	5.28	21	84
		60	24.9	100	
TMA-GeW_{11}-Pt-NH_3		15	12.97	52	208
		60	20.0	116	
TMA-AlW_{11}-Pt-NH_3		15	10.97	44	176
		60	20.6	82	
TMA-BW_{11}-Pt-NH_3		15	3.28	13	52
		60	20.2	81	
Cs-GeW_{11}-Pt-bpy		15	0.73	3	12
		60	2.84	11	
Cs-GeW_{11}-Pt-phen		15	1.07	4	16
		60	5.01	20	
Cs-P_2W_{17}-Pt-NH_3		15	31.8	127	508
		60	57.2	229	
TMA-PW_{11}-Pt-NH_3	2.0	15	29.4	29	116
		60	77.0	77	
TMA-SiW_{11}-Pt-NH_3		15	14.0	14	56
		60	38.3	38	
TMA-GeW_{11}-Pt-NH_3		15	20.1	20	80
		60	50.4	50	
TMA-AlW_{11}-Pt-NH_3		15	15.2	15	60
		60	41.0	41	
TMA-BW_{11}-Pt-NH_3		15	8.9	9	36
		60	35.0	35	
Cs-GeW_{11}-Pt-bpy		15	2.60	3	12
		60	2.93	3	
Cs-GeW_{11}-Pt-phen		15	–	–	–
		60			
Cs-P_2W_{17}-Pt-NH_3		15	43.7	44	176
		60	135.3	135	

[a] Reaction conditions: platinum compound (0.5 and 2.0 μmol Pt), EY (2.5 μmol), 100 mM TEOA aq. soln. (10 mL; pH 7), 25 °C, light irradiation (λ = ≥400 nm).

[b] Turnover number (TON) = 2[H_2 evolved (mol)]/[Pt atom (mol)].

[c] Turnover frequency (TOF) = TON/h after 15 min.

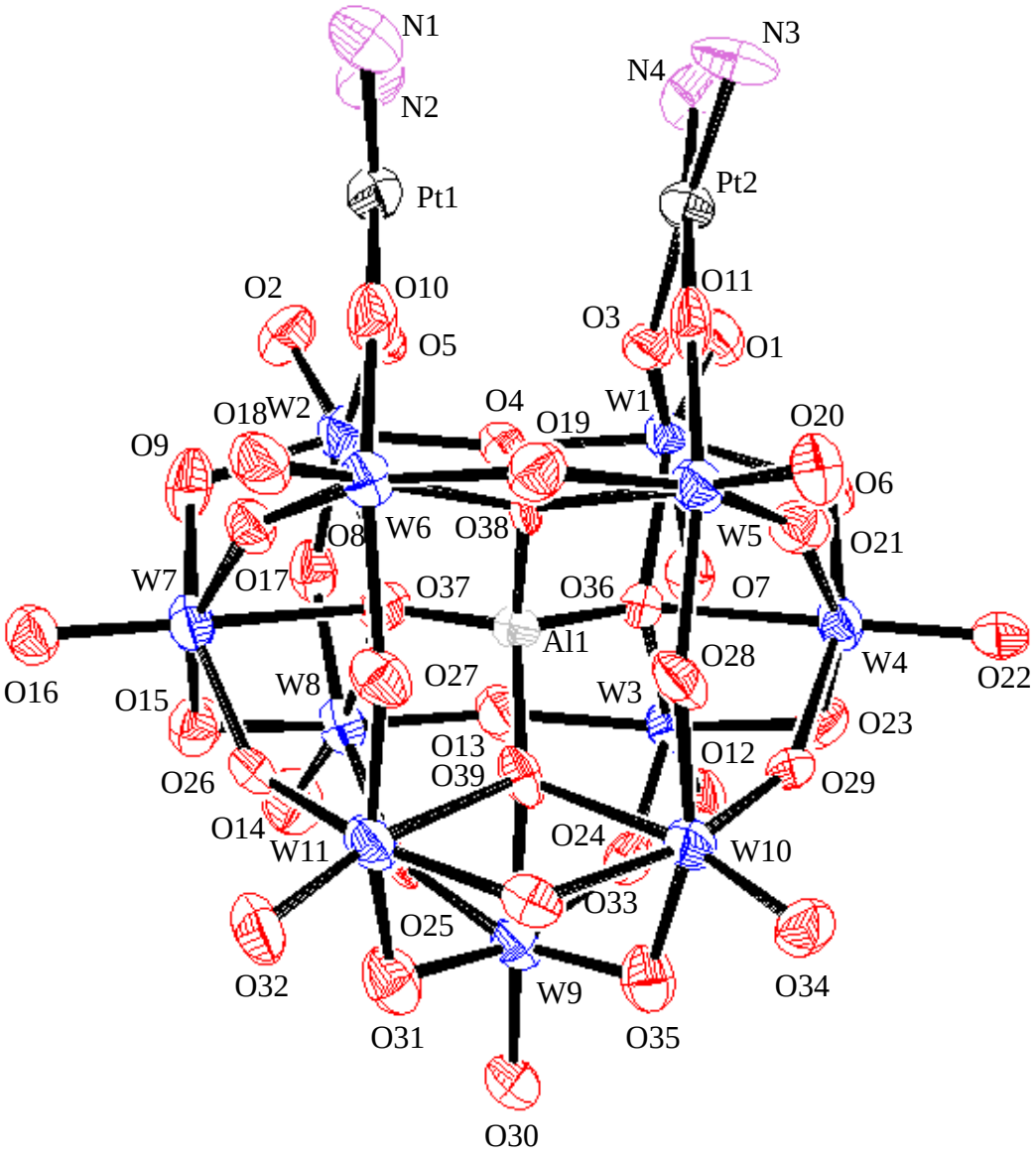
N1
N2
Pt1
N3
N4
Pt2
O2
O10
O5
O3
O11
O1
O18
W2
O4
O19
W1
O20
O9
O6
O8
W6
O38
W5
O21
W7
O17
O37
O36
O7
Al1
O16
O15
W8
O27
O28
W4
O22
W3
O23
O13
O12
O26
O39
O29
O14
W11
O24
W10
O33
O25
O32
W9
O34
O31
O35
O30

Fig. 1

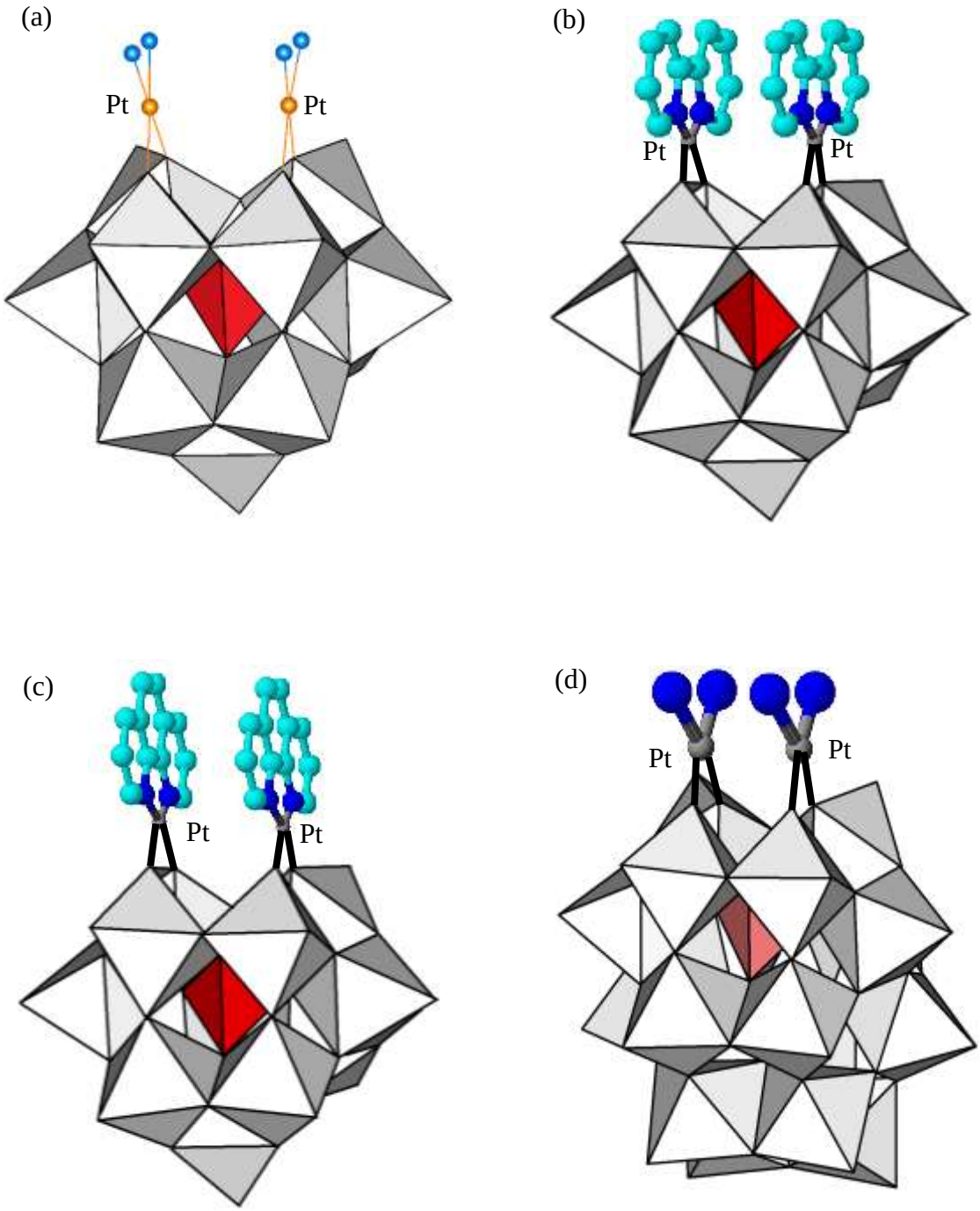

Fig. 2

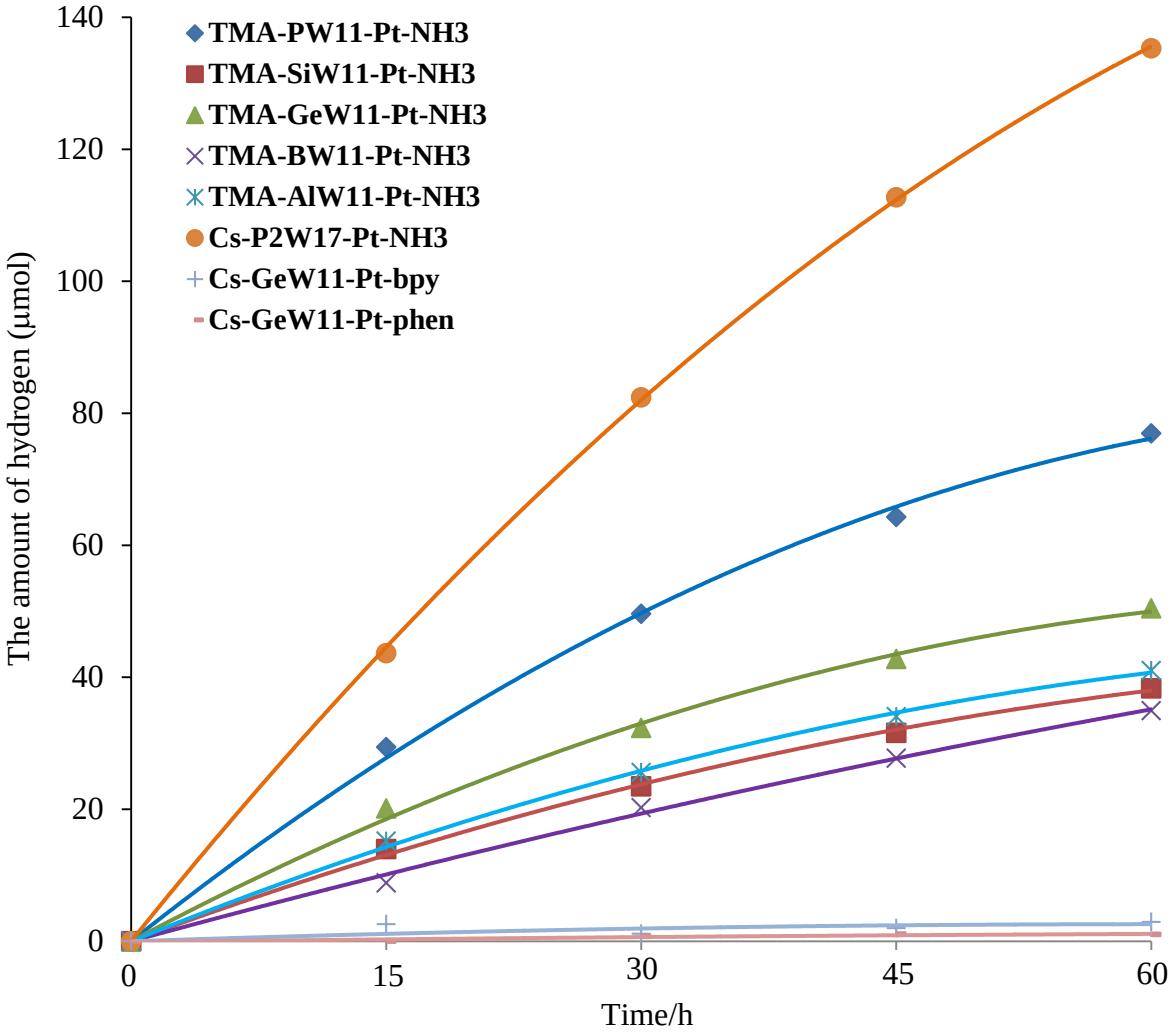
TMA-PW11-Pt-NH3
TMA-SiW11-Pt-NH3
TMA-GeW11-Pt-NH3
TMA-BW11-Pt-NH3
TMA-AlW11-Pt-NH3
Cs-P2W17-Pt-NH3
Cs-GeW11-Pt-bpy
Cs-GeW11-Pt-phen
The amount of hydrogen (μmol)
140
120
100
80
60
40
20
0
0
15
30
45
60
Time/h

Fig. 3

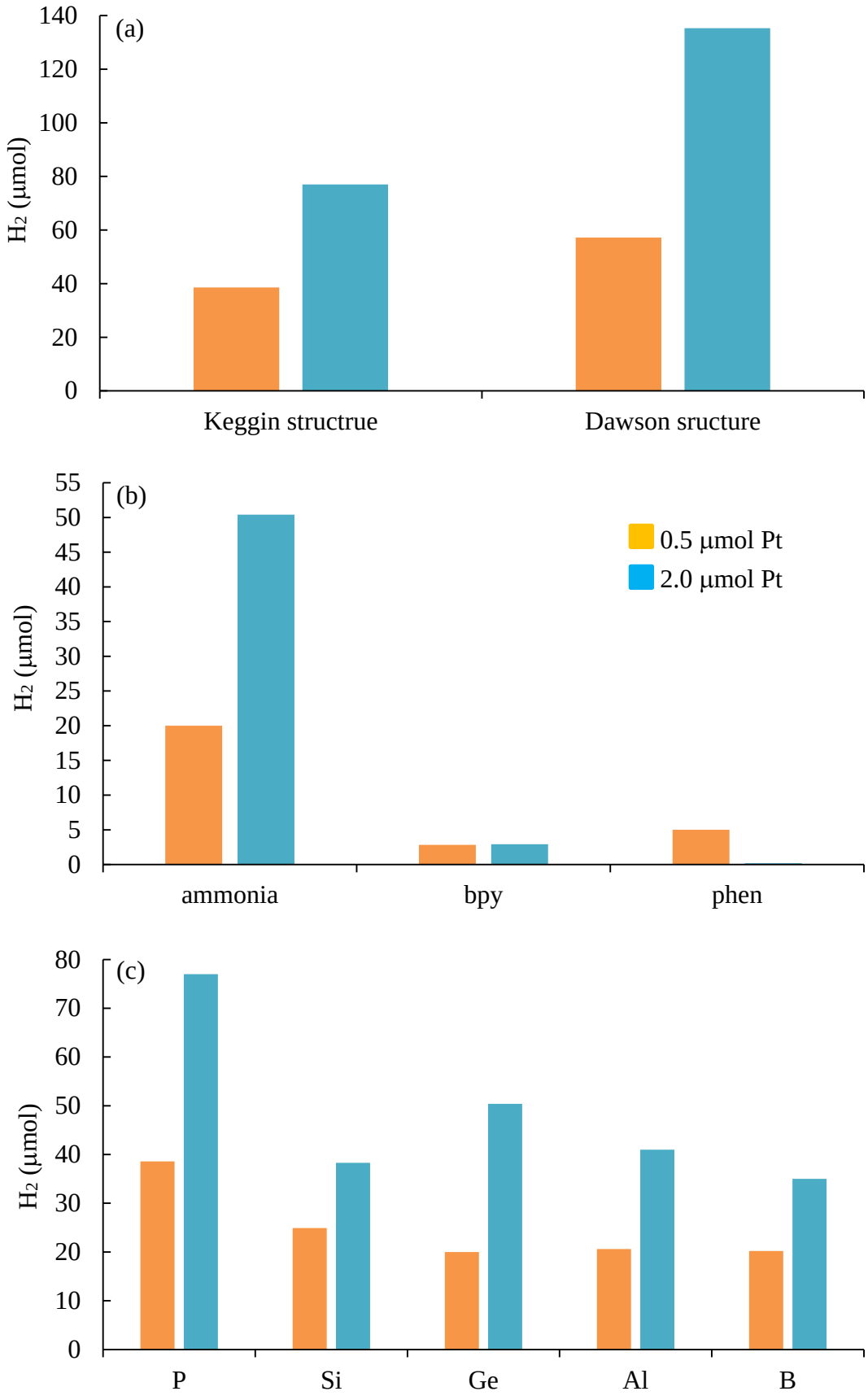
(a)
H₂ (μmol)
140
120
100
80
60
40
20
0
Keggin structrue
Dawson sructure
(b)
H₂ (μmol)
55
50
45
40
35
30
25
20
15
10
5
0
0.5 μmol Pt
2.0 μmol Pt
ammonia
bpy
phen
(c)
H₂ (μmol)
80
70
60
50
40
30
20
10
0
P
Si
Ge
Al
B

Fig. 4

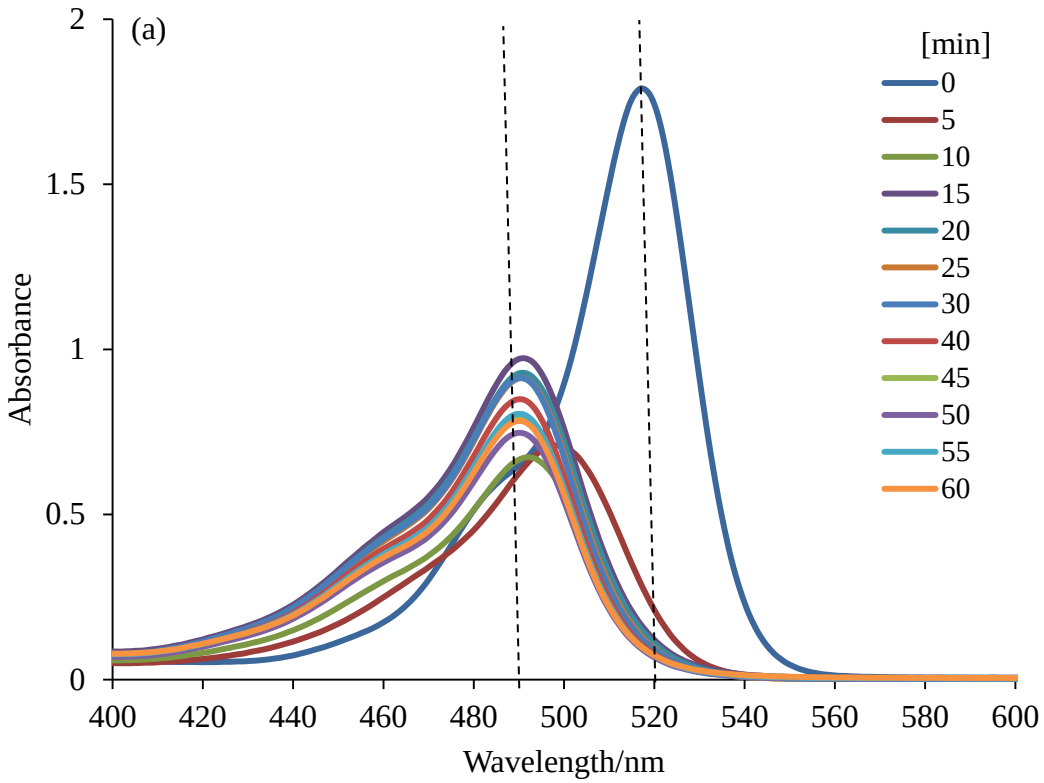
(a)
[min]
0
5
10
15
20
25
30
40
45
50
55
60
Absorbance
Wavelength/nm
2
1.5
1
0.5
0
400
420
440
460
480
500
520
540
560
580
600

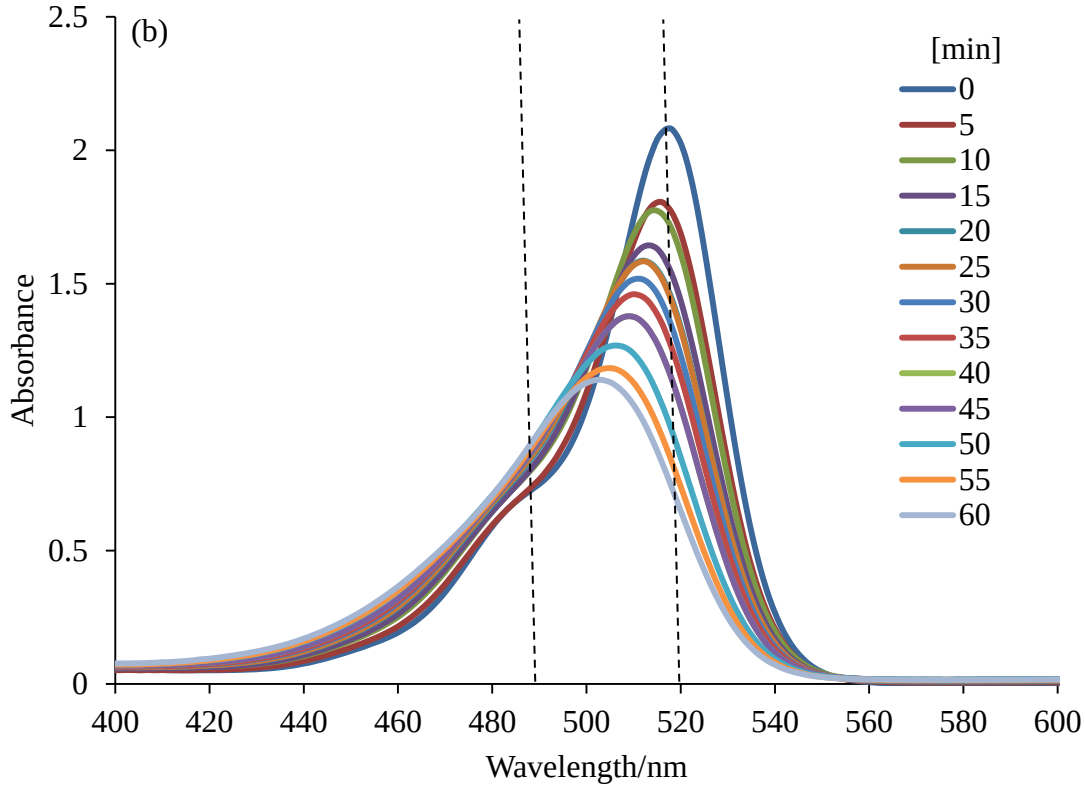
(b)
[min]
0
5
10
15
20
25
30
35
40
45
50
55
60
Absorbance
Wavelength/nm
2.5
2
1.5
1
0.5
0
400
420
440
460
480
500
520
540
560
580
600

Fig. 5

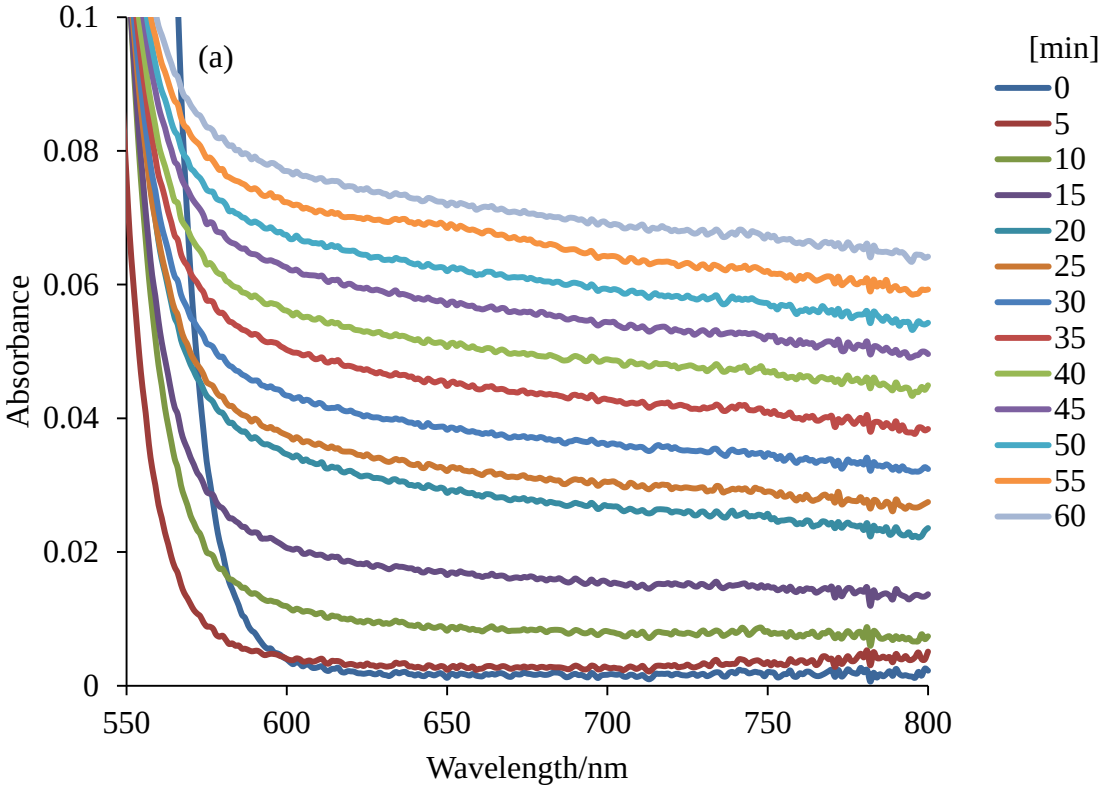
(a)
Absorbance
0.1
0.08
0.06
0.04
0.02
0
550
600
650
700
750
800
Wavelength/nm
[min]
0
5
10
15
20
25
30
35
40
45
50
55
60

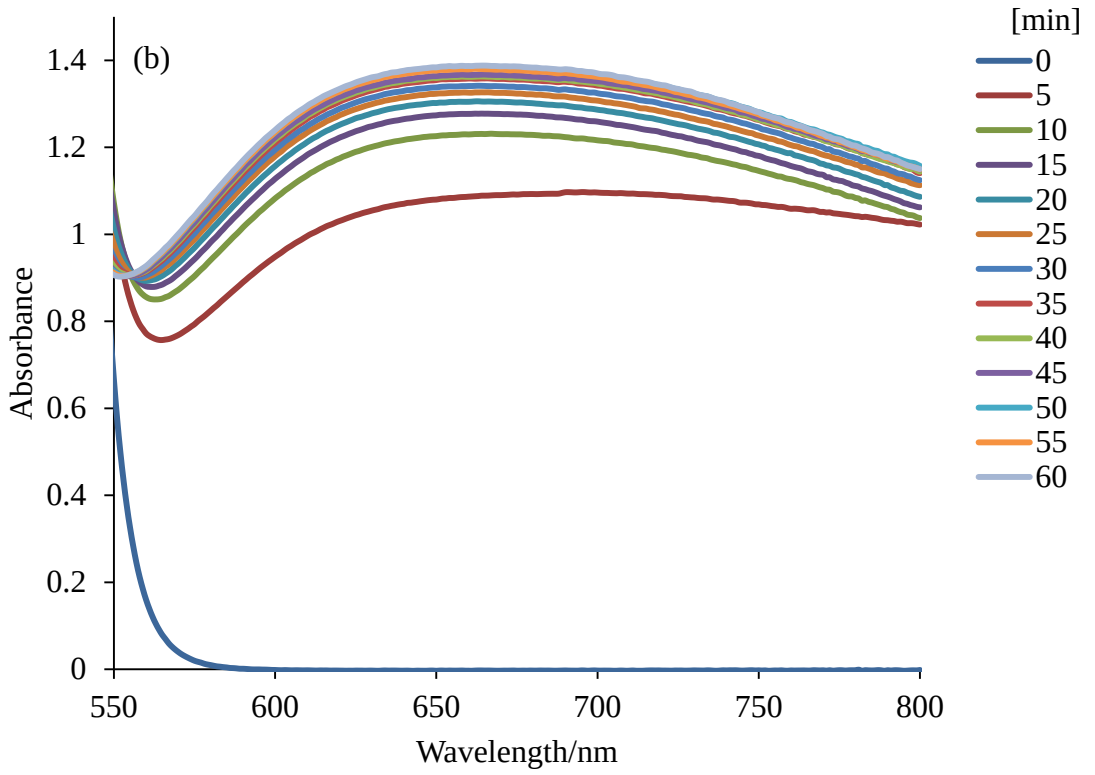
(b)
Absorbance
1.4
1.2
1
0.8
0.6
0.4
0.2
0
550
600
650
700
750
800
Wavelength/nm
[min]
0
5
10
15
20
25
30
35
40
45
50
55
60

Fig. 6